

扫描二维码  
查看更多

## miR-154-5p 对肺癌骨转移的影响研究

常琪<sup>1</sup>, 马飒飒<sup>1</sup>, 李占标<sup>1</sup>, 袁欣<sup>1</sup>, 孙静茹<sup>2</sup>

作者单位: 1.252000山东省聊城市人民医院疼痛科 2.252000山东省聊城市人民医院质控科

通信作者: 孙静茹, E-mail: stney2009@163.com

**【摘要】** 目的 探讨miR-154-5p对肺癌骨转移的影响。方法 本实验时间为2021年9月—2022年2月。选取BALB/c-nu小鼠60只,采用随机数字表法将小鼠分为载体组和miR-154-5p组,每组30只。将pMSCV puro反转录病毒载体或过表达miR-154-5p的A549细胞分别注入载体组、miR-154-5p组小鼠左心室。注药第80天,载体组剩余6只存活,miR-154-5p组剩余21只存活。载体组取6只小鼠,miR-154-5p组随机取6只小鼠,用于后期数据分析。注药第0、20、40、60、80天采用缩爪阈值评估小鼠机械性疼痛程度,注药第80天进行X线检查以评价小鼠骨转移评分,注药第80天采用苏木精-伊红染色检测溶骨性病损面积。从注药开始每天监测两组小鼠生存情况,并记录80 d。结果 干预方法与时间在缩爪阈值上存在交互作用( $P < 0.05$ ),干预方法、时间在缩爪阈值上主效应显著( $P < 0.05$ );注药第40、60、80天,miR-154-5p组缩爪阈值高于载体组( $P < 0.05$ )。注药第80天,miR-154-5p组骨转移评分低于载体组,溶骨性病损面积小于载体组( $P < 0.05$ )。载体组生存率为20%,miR-154-5p组生存率为70.0%。miR-154-5p组生存率高于载体组( $P < 0.05$ )。载体组中位无骨转移生存期为35 d,无骨转移生存率为86.7%;miR-154-5p组中位无骨转移生存期为76 d,无骨转移生存率为50.0%。miR-154-5p组无骨转移生存率高于载体组( $P < 0.05$ )。结论 miR-154-5p上调可提高肺癌小鼠的缩爪阈值,抑制骨转移,并延长小鼠生存期和无骨转移生存期。

**【关键词】** 肺肿瘤; 肿瘤转移; 骨转移; miR-154-5p**【中图分类号】** R 734.2 **【文献标识码】** A DOI: 10.12114/j.issn.1008-5971.2024.00.098

### Effect of miR-154-5p on Bone Metastasis in Lung Cancer

CHANG Qi<sup>1</sup>, MA Sasa<sup>1</sup>, LI Zhanbiao<sup>1</sup>, YUAN Xin<sup>1</sup>, SUN Jingru<sup>2</sup>

1.Department of Pain, Liaocheng People's Hospital, Liaocheng 252000, China

2.Quality Control Department, Liaocheng People's Hospital, Liaocheng 252000, China

Corresponding author: SUN Jingru, E-mail: stney2009@163.com

**【Abstract】 Objective** To investigate the effect of miR-154-5p on bone metastasis in lung cancer. **Methods** Experimental time of this study was from September 2021 to February 2022. Sixty BALB/c-nu mice were selected and divided into carrier group and miR-154-5p group using a random number table method, with 30 mice in each group. The pMSCV puro retrovirus vector or A549 cells overexpressing miR-154-5p were injected into the left ventricle of mice in carrier group and miR-154-5p group, respectively. On the 80th day of drug injection, 6 mice in the carrier group survived and 21 mice in the miR-154-5p group survived. Six mice were selected from the carrier group and six mice were randomly selected from the miR-154-5p group for later data analysis. On the 0th, 20th, 40th, 60th and 80th day of drug injection, the degree of mechanical pain in mice was evaluated by paw withdrawal threshold; on the 80th day of drug injection, the bone metastasis score was evaluated by X-ray examination, and the osteolytic lesion area was detected by hematoxylin eosin staining. The survival and bone metastasis-free survival of mice were monitored every day for 80 days. **Results** There was an interaction between intervention methods and time on the paw withdrawal threshold ( $P < 0.05$ ), both intervention methods and time produced significant main effects on the paw withdrawal threshold ( $P < 0.05$ ). On the 40th, 60th and 80th day of drug injection, the paw withdrawal threshold in miR-154-5p group was higher than that in carrier group ( $P < 0.05$ ). On the 80th day of drug injection, the bone metastasis score in miR-154-5p group was lower than that in carrier group, and osteolytic lesion area was smaller than that in carrier group ( $P < 0.05$ ). The overall survival rate of carrier group was 20.0%, the overall survival rate of miR-154-5p group was 70.0%. The survival rate in miR-154-5p group was higher than that in carrier group ( $P < 0.05$ ). The median bone metastasis-free survival time in the carrier group was 35 days, and the bone metastasis-free survival rate was 86.7%. The median bone metastasis-free survival time in the

miR-154-5p group was 76 days, and the bone metastasis-free survival rate was 50.0%. The bone metastasis-free survival rate in miR-154-5p group was higher than that in carrier group ( $P < 0.05$ ). **Conclusion** Upregulation of miR-154-5p can increase the paw withdrawal threshold of lung cancer mice, reduce the bone metastasis, and prolong the survival time and bone metastasis-free survival time.

**【 Key words 】** Lung neoplasms; Neoplasm metastasis; Bone metastasis; miR-154-5p

肺癌是全球癌症相关死亡的主要原因, 其中50%~70%的患者发生骨转移<sup>[1-2]</sup>。骨转移在肺癌终末期患者中更为常见, 患者常出现严重的癌性骨痛, 进而严重影响其生活质量<sup>[3]</sup>。由于癌性骨痛的不良预后, 需要进一步探索肺癌细胞增殖、侵袭、转移的潜在机制<sup>[3]</sup>。微小RNA (microRNA, miRNA) 是内源性小的非编码的高度保守的RNAs<sup>[4]</sup>。研究表明, miRNA功能障碍参与了恶性肿瘤的发生和发展, 如乳腺癌、子宫内膜癌、胃癌、前列腺癌和肺癌<sup>[5-6]</sup>。此外, 研究证明, miRNA与骨转移瘤相关<sup>[7]</sup>。还有研究表明, miR-154-5p在恶性肿瘤中下调, 而miR-154-5p过表达可能在抑制肿瘤发生中发挥潜在作用<sup>[8]</sup>。值得注意的是, 先前有学者使用miRCURY LNA microRNA阵列确定了miR-154-5p是肺癌相关的潜在生物标志物, 并且miR-154-5p在抑制肿瘤发生中起主要作用<sup>[9-11]</sup>。然而, 目前研究尚不清楚miR-154-5p是否参与肺癌骨转移的发生。基于此, 本研究旨在探讨miR-154-5p对肺癌骨转移的影响, 现报道如下。

## 1 材料与方法

### 1.1 实验动物

实验时间: 2021年9月—2022年2月。选取BALB/c-nu小鼠60只, 雌雄各半, 5~6周龄, 体质量18~20 g, 购自上海斯莱克实验动物有限责任公司。置于温控室内、12 h/12 h的光/暗交替环境下饲养。所有小鼠允许自由饮食、饮水。本研究经聊城市人民医院伦理委员会批准同意 (审批号: 伦审2021-013)。

### 1.2 仪器与试剂

pMSCV puro反转录病毒载体购自日本Clontech公司, Lipofectamine 2000购自美国Invitrogen公司, vonfery机械刺痛测试包购自上海软隆科技发展有限公司, Metamorph图像分析系统和软件购自美国Universal Imaging Corporation公司。

### 1.3 载体与转染

A549细胞 (肺癌人类肺泡基底上皮细胞) 购自中国科学院典型培养物保藏委员会细胞库。A549细胞在含95%空气和5% CO<sub>2</sub>的37 °C加湿环境的培养箱中培养。人miR-154-5p基因通过PCR从基因组DNA中扩增, 并克隆到pMSCV puro反转录病毒载体中。使用Lipofectamine 2000将扩增的miR-154-5p质粒转染到A549细胞中, 制备过表达miR-154-5p的A549细胞。

### 1.4 模型制备

采用随机数字表法将小鼠分为载体组和miR-154-5p组, 每组30只。两组小鼠腹腔注射0.3%戊巴比妥钠麻醉, 将100 μl pMSCV puro反转录病毒载体、过表达miR-154-5p的A549细胞 (细胞总量为 $1 \times 10^5$  cells/ml, 溶于100 μl PBS) 分别注入载体组、miR-154-5p组小鼠左心室。注药第80天, 载体组剩余6只存活, miR-154-5p组剩余21只存活。载体组取6只小鼠, miR-154-5p组随机取6只小鼠, 用于后期数据分析。

### 1.5 缩爪阈值评估

分别于注药第0、20、40、60、80天, 采用缩爪阈值来评估小鼠机械性疼痛程度。将小鼠置于带有金属网的透明笼子中, 用von Frey纤维丝刺激小鼠后爪。每只小鼠测试5次, 最小刺激强度和诱导缩爪的最低von Frey纤维丝被认为是缩爪阈值。缩爪阈值 (g) =  $[10 (Xf + k \delta)] / 10\ 000$ , 其中Xf为最后一根von Frey纤维丝编号,  $\delta$  为所取各根von Frey纤维丝取对数后的均差, 约等于0.224, k为根据测量获得的“阳性反应”“阴性反应”序列查表后获得的系数值。

### 1.6 骨转移评分评估

注药第80天, 对小鼠腹腔注射0.3%戊巴比妥钠以麻醉小鼠, 将小鼠四肢伸展, 用胶条固定, 进行X线检查。根据以下标准进行骨转移评分评估: 无转移为0分; 骨病变累及骨宽度 $< 1/4$ 为1分; 骨病变累及骨宽度的 $1/4 \sim 1/2$ 为2分; 骨病变累及骨宽度 $> 1/2 \sim 3/4$ 为3分; 骨病变累及骨宽度 $> 3/4$ 为4分<sup>[10]</sup>。每只小鼠的骨转移评分为四肢骨转移评分的总和。

### 1.7 溶骨性病变面积测量

注药第80天, 采用颈椎脱臼法处死小鼠。获得小鼠胫骨, 在4 °C下固定, 将样本包埋在石蜡中并对转移骨组织进行切片、脱蜡、苏木精-伊红染色, 使用Metamorph图像分析系统和软件测量溶骨性病变面积。

### 1.8 预后观察

从注药开始每天监测两组小鼠生存情况, 连续记录80 d。

### 1.9 统计学方法

采用GraphPad 9.5.0统计学软件进行数据分析。计量资料以 $(\bar{x} \pm s)$ 表示, 重复测量数据比较采用双因素重复测量方差分析, 两组间比较采用成组t检验; 绘制生存期及无骨转移生存期的生存曲线, 比较采用Log-

rank检验。以 $P < 0.05$ 为差异有统计学意义。

## 2 结果

### 2.1 缩爪阈值

干预方法与时间在缩爪阈值上存在交互作用 ( $P < 0.05$ )，干预方法、时间在缩爪阈值上主效应显著 ( $P < 0.05$ )；注药第40、60、80天，miR-154-5p组缩爪阈值高于载体组，差异有统计学意义 ( $P < 0.05$ )，见表1。

### 2.2 骨转移评分、溶骨性病变更面积

注药第80天，miR-154-5p组骨转移评分低于载体组，溶骨性病变更面积小于载体组，差异有统计学意义 ( $P < 0.05$ )，见表2、图1~2。

表1 两组小鼠不同时间缩爪阈值比较 ( $\bar{x} \pm s$ , g,  $n=6$ )

Table 1 Comparison of paw withdrawal threshold between the two groups at different time

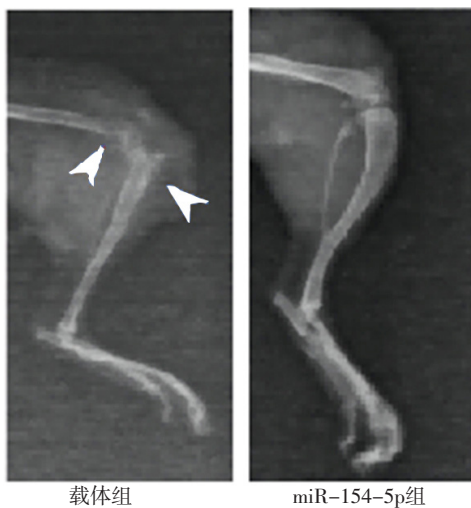
组别	注药第0天	注药第20天	注药第40天	注药第60天	注药第80天
载体组	15.22 ± 0.57	12.11 ± 1.03	9.08 ± 1.14	5.31 ± 0.89	3.55 ± 0.42
miR-154-5p组	15.01 ± 0.48	14.20 ± 0.78	14.07 ± 0.82*	13.52 ± 1.93*	13.04 ± 0.92*
F值	$F_{交互}=197.40, F_{组间}=362.70, F_{时间}=365.80$				
P值	$P_{交互}<0.001, P_{组间}<0.001, P_{时间}<0.001$				

注：\*表示与载体组比较， $P < 0.05$ 。

表2 两组骨转移评分、溶骨性病变更面积比较 ( $\bar{x} \pm s$ ,  $n=6$ )

Table 2 Comparison of bone metastasis score and osteolytic lesion area between the two groups

组别	骨转移评分 (分)	溶骨性病变更面积 ( $\text{mm}^2$ )
载体组	8.92 ± 0.53	7.72 ± 0.51
miR-154-5p组	1.23 ± 0.08	2.23 ± 0.18
t值	36.32	24.59
P值	<0.001	<0.001



注：箭头所指为溶骨性病变更。

图1 载体组与miR-154-5p组小鼠骨转移X线检查图像

Figure 1 X-ray examination images of bone metastasis in mice of carrier group and miR-154-5p group

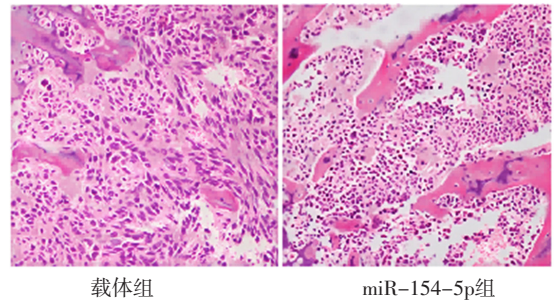


图2 载体组与miR-154-5p组小鼠胫骨中骨溶骨区的组织形态学 (苏木精-伊红染色,  $\times 100$ )

Figure 2 Histomorphology of osteolytic region in tibia of mice in carrier group and miR-154-5p group

### 2.3 预后

载体组生存率为20.0%，miR-154-5p组生存率为70.0%。miR-154-5p组生存率高于载体组，差异有统计学意义 ( $\chi^2=15.99, P < 0.001$ )，见图3。载体组中位无骨转移生存期为35 d，无骨转移生存率为86.7%；miR-154-5p组中位无骨转移生存期为76 d，无骨转移生存率为50.0%。miR-154-5p组无骨转移生存率高于载体组，差异有统计学意义 ( $\chi^2=19.44, P < 0.001$ )，见图4。

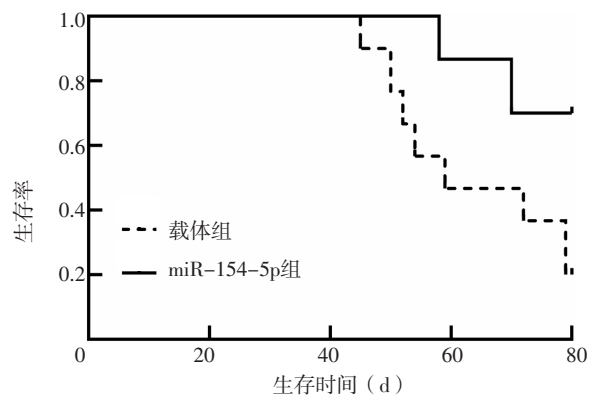


图3 载体组与miR-154-5p组小鼠生存曲线

Figure 3 Survival curve of carrier group and miR-154-5p group

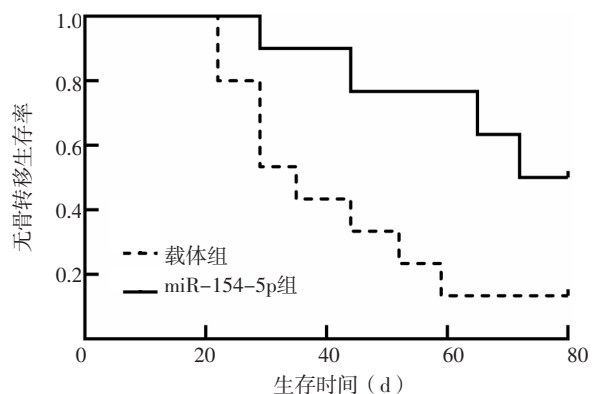


图4 载体组与miR-154-5p组小鼠无骨转移生存曲线

Figure 4 Bone metastasis-free survival curve of carrier group and miR-154-5p group

### 3 讨论

癌症骨转移是一个多步骤的过程,表现出一系列独特的骨骼并发症,包括骨痛、病理性骨折、高钙血症和脊髓压迫。在此过程中,侵袭性肿瘤细胞可能会在上皮间质转化和原发性肿瘤微环境的促进下以单循环肿瘤细胞的形式侵入血管;在血液循环中,单循环肿瘤细胞与血小板聚集并黏附于骨髓内皮,然后外渗到骨髓实质中;一旦骨髓中的肿瘤细胞由于某些有利条件而从休眠状态重新激活,就会形成微转移并最终导致明显转移<sup>[12]</sup>。骨转移可分为成骨性转移和溶骨性转移,大多数非小细胞肺癌骨转移为溶骨性骨转移<sup>[13]</sup>。癌症骨转移可引起剧烈疼痛、病理性骨折和脊髓压迫,进而严重影响患者的生活质量。尽管目前癌症骨痛相关研究已经取得了一些临床进展,但其仍然是临床医生面临的重要挑战。

近年越来越多的证据表明,miRNA可参与恶性肿瘤细胞增殖、迁移和侵袭,包括肺癌骨转移<sup>[7, 14]</sup>。研究表明,miR-154-5p在胃癌、转移性肝癌和霍奇金淋巴瘤患者中表达降低,并且miR-154-5p的下调通过不同机制参与肿瘤的发生和转移<sup>[15-16]</sup>。研究报道,miR-154-5p在转移性前列腺癌中表达下调,其与前列腺癌细胞转移相关<sup>[17]</sup>。对于miR-154-5p在肺癌中的作用,一项生信分析报道了肺癌患者血清miR-154-5p水平降低,并且miR-154-5p水平可作为肺癌早期检测和预后预测的生物标志物<sup>[18]</sup>。此外,还有研究报道,miR-154-5p可作为神经病理性疼痛的治疗靶点,下调脊髓组织中miR-154-5p表达水平可加重慢性狭窄损伤大鼠神经病理性疼痛程度<sup>[19]</sup>。本研究结果显示,注药第40、60、80天,miR-154-5p组缩爪阈值高于载体组;注药第80天,miR-154-5p组骨转移评分、溶骨性病变更面积低于载体组,同时,miR-154-5p组生存率、无骨转移生存率高于载体组,提示miR-154-5p过表达可抑制肺癌小鼠骨转移,延长小鼠无骨转移生存期。研究显示,miR-154-5p在肺癌骨转移中具有肿瘤抑制作用,并有助于减轻癌症骨痛<sup>[20-21]</sup>。

### 4 结论

综上所述,miR-154-5p上调可提高肺癌小鼠的缩爪阈值,抑制骨转移,并延长小鼠生存期和无骨转移生存期。miR-154-5p可能是肺癌骨转移的一个有前景的治疗靶点。然而,本研究并未进一步探讨miR-154-5p可能的作用机制。

作者贡献:常琪、马飒飒进行文章的构思与设计;孙静茹进行研究的实施与可行性分析,负责文章的质量控制及审校,对文章整体负责、监督管理;李占标进行资料收集;常琪、李占标进行资料整理;常琪撰写论文;袁欣负责统计学处理;常琪、孙静茹进行论文的

修订。

本文无利益冲突。

### 参考文献

- [1] WU S Y, PAN Y, MAO Y Y, et al. Current progress and mechanisms of bone metastasis in lung cancer: a narrative review [J]. *Transl Lung Cancer Res*, 2021, 10 (1): 439-451. DOI: 10.21037/tlcr-20-835.
- [2] 数据“说”癌症 [J]. *实用心脑血管病杂志*, 2023, 31 (5): 4.
- [3] DA SILVA G T, BERGMANN A, THULER L C S. Incidence and risk factors for bone metastasis in non-small cell lung cancer [J]. *Asian Pac J Cancer Prev*, 2019, 20 (1): 45-51. DOI: 10.31557/APJCP.2019.20.1.45.
- [4] BELLAVIA D, SALAMANNA F, RAIMONDI L, et al. Deregulated miRNAs in osteoporosis: effects in bone metastasis [J]. *Cell Mol Life Sci*, 2019, 76 (19): 3723-3744. DOI: 10.1007/s00018-019-03162-w.
- [5] 孟圆圆, 迟鹏宇, 马丽辉, 等. 子宫内膜癌组织微小RNA-373表达情况及其对子宫内膜癌细胞增殖、迁移的影响研究 [J]. *实用心脑血管病杂志*, 2020, 28 (3): 82-87. DOI: 10.3969/j.issn.1008-5971.2020.03.017.
- [6] UZUNER E, ULU G T, GÜRLER S B, et al. The role of MiRNA in cancer: pathogenesis, diagnosis, and treatment [J]. *Methods Mol Biol*, 2022, 2257: 375-422. DOI: 10.1007/978-1-0716-1170-8\_18.
- [7] LANG J L, ZHAO Q, HE Y D, et al. Bone turnover markers and novel biomarkers in lung cancer bone metastases [J]. *Biomarkers*, 2018, 23 (6): 518-526. DOI: 10.1080/1354750X.2018.1463566.
- [8] JIANG J C, CHENG X Q. Circular RNA circABCC4 acts as a ceRNA of miR-154-5p to improve cell viability, migration and invasion of breast cancer cells in vitro [J]. *Cell Cycle*, 2020, 19 (20): 2653-2661. DOI: 10.1080/15384101.2020.1815147.
- [9] ZHOU C W, CHEN Z X, ZHAO L L, et al. A novel circulating miRNA-based signature for the early diagnosis and prognosis prediction of non-small-cell lung cancer [J]. *J Clin Lab Anal*, 2020, 34 (11): e23505. DOI: 10.1002/jcla.23505.
- [10] 赵亮, 富凯丽, 姚兰琳, 等. 整合素 $\alpha v\beta 3$ 放射性核素靶向治疗联合PD-L1免疫治疗的实验研究 [J]. *中华核医学与分子影像杂志*, 2020, 40 (5): 268-274. DOI: 10.3760/cma.j.cn321828-20191128-00278.
- [11] KWAKWA K A, STERLING J A. Integrin  $\alpha v\beta 3$  signaling in tumor-induced bone disease [J]. *Cancers*, 2017, 9 (7): 84. DOI: 10.3390/cancers9070084.
- [12] YANG X R, PI C, YU R Y, et al. Correlation of exosomal microRNA clusters with bone metastasis in non-small cell lung cancer [J]. *Clin Exp Metastasis*, 2021, 38 (1): 109-117. DOI: 10.1007/s10585-020-10062-y.
- [13] CLÉZARDIN P, COLEMAN R, PUPPO M, et al. Bone metastasis: mechanisms, therapies, and biomarkers [J]. *Physiol Rev*, 2021, 101 (3): 797-855. DOI: 10.1152/physrev.00012.2019.

- [14] ZHANG J, WU J M. The potential roles of exosomal miR-214 in bone metastasis of lung adenocarcinoma [J]. *Front Oncol*, 2021, 10: 611054. DOI: 10.3389/fonc.2020.611054.
- [15] CHEN K, ZHANG Z Q, YU A J, et al. lncRNA DLGAP1-AS2 knockdown inhibits hepatocellular carcinoma cell migration and invasion by regulating miR-154-5p methylation [J]. *Biomed Res Int*, 2020, 2020: 6575724. DOI: 10.1155/2020/6575724.
- [16] NAZARIZADEH A, MOHAMMADI F, ALIAN F, et al. MicroRNA-154: a novel candidate for diagnosis and therapy of human cancers [J]. *Onco Targets Ther*, 2020, 13: 6603-6615. DOI: 10.2147/OTT.S249268.
- [17] FREDSTØE J, RASMUSSEN A K I, MOURITZEN P, et al. Profiling of circulating microRNAs in prostate cancer reveals diagnostic biomarker potential [J]. *Diagnostics*, 2020, 10 (4): 188. DOI: 10.3390/diagnostics10040188.
- [18] ZHOU C W, CHEN Z X, ZHAO L L, et al. A novel circulating miRNA-based signature for the early diagnosis and prognosis prediction of non-small-cell lung cancer [J]. *J Clin Lab Anal*, 2020, 34 (11): e23505. DOI: 10.1002/jcla.23505.
- [19] WU J P, WANG C G, DING H Y. LncRNA MALAT1 promotes neuropathic pain progression through the miR-154-5p/AQP9 axis in CCI rat models [J]. *Mol Med Rep*, 2020, 21 (1): 291-303. DOI: 10.3892/mmr.2019.10829.
- [20] HONG S P, CHAN T E, LOMBARDO Y, et al. Single-cell transcriptomics reveals multi-step adaptations to endocrine therapy [J]. *Nat Commun*, 2019, 10 (1): 3840. DOI: 10.1038/s41467-019-11721-9.
- [21] WANG L, SONG L J, LI J, et al. Bone sialoprotein- $\alpha$  v  $\beta$  3 integrin axis promotes breast cancer metastasis to the bone [J]. *Cancer Sci*, 2019, 110 (10): 3157-3172. DOI: 10.1111/cas.14172.
- (收稿日期: 2023-11-12; 修回日期: 2024-03-28)  
(本文编辑: 陈素芳)

(上接第77页)

- [25] RAMOS-FERNANDEZ M, BELLOLIO M F, STEAD L G. Matrix metalloproteinase-9 as a marker for acute ischemic stroke: a systematic review [J]. *J Stroke Cerebrovasc Dis*, 2011, 20 (1): 47-54. DOI: 10.1016/j.jstrokecerebrovasdis.2009.10.008.
- [26] WANG L, WEI C C, DENG L H, et al. The accuracy of serum matrix metalloproteinase-9 for predicting hemorrhagic transformation after acute ischemic stroke: a systematic review and meta-analysis [J]. *J Stroke Cerebrovasc Dis*, 2018, 27 (6): 1653-1665. DOI: 10.1016/j.jstrokecerebrovasdis.2018.01.023.
- [27] ZHONG Y, YIN B, YE Y Z, et al. The bidirectional role of the JAK2/STAT3 signaling pathway and related mechanisms in cerebral ischemia-reperfusion injury [J]. *Exp Neurol*, 2021, 341: 113690. DOI: 10.1016/j.expneurol.2021.113690.
- [28] BALIC J J, ALBARGY H, LUU K, et al. STAT3 serine phosphorylation is required for TLR4 metabolic reprogramming and IL-1 $\beta$  expression [J]. *Nat Commun*, 2020, 11 (1): 3816. DOI: 10.1038/s41467-020-17669-5.
- [29] BORBOR M, YIN D P, BROCKMEIER U, et al. Neurotoxicity of ischemic astrocytes involves STAT3-mediated metabolic switching and depends on glycogen usage [J]. *Glia*, 2023, 71 (6): 1553-1569. DOI: 10.1002/glia.24357.
- [30] FAGERHOLM S C, MACPHERSON M, JAMES M J, et al. The CD11b-integrin (ITGAM) and systemic lupus erythematosus [J]. *Lupus*, 2013, 22 (7): 657-663. DOI: 10.1177/0961203313491851.
- [31] KHAN S Q, KHAN I, GUPTA V. CD11b activity modulates pathogenesis of lupus nephritis [J]. *Front Med*, 2018, 5: 52. DOI: 10.3389/fmed.2018.00052.
- [32] LIU R, XU N G, YI W, et al. Electroacupuncture attenuates inflammation after ischemic stroke by inhibiting NF- $\kappa$ B-mediated activation of microglia [J]. *Evid Based Complement Alternat Med*, 2020, 2020: 8163052. DOI: 10.1155/2020/8163052.
- [33] HU W B, LIU L, FORN-CUNÍ G, et al. Transcriptomic and metabolomic studies reveal that toll-like receptor 2 has a role in glucose-related metabolism in unchallenged zebrafish larvae (*Danio rerio*) [J]. *Biology*, 2023, 12 (2): 323. DOI: 10.3390/biology12020323.
- [34] FENG T T, YANG X Y, HAO S S, et al. TLR-2-mediated metabolic reprogramming participates in polyene phosphatidylcholine-mediated inhibition of M1 macrophage polarization [J]. *Immunol Res*, 2020, 68 (1): 28-38. DOI: 10.1007/s12026-020-09125-9.
- (收稿日期: 2023-11-23; 修回日期: 2024-01-24)  
(本文编辑: 崔丽红)